Polymer 51 (2010) 647–654

Contents lists available at ScienceDirect

Polymer

journal homepage: www.elsevier.com/locate/polymer

Phase separation in polymer blend thin films studied by differential AC chip calorimetry

Nicolaas-Alexander Gotzen [a], Heiko Huth [b], Christoph Schick [b], Guy Van Assche [a], Carine Neus [c], Bruno Van Mele [a,*]

[a] Vrije Universiteit Brussel, Department of Materials and Chemistry (MACH), Research Unit Physical Chemistry and Polymer Science (FYSC), Pleinlaan 2, B-1050 Brussels, Belgium
[b] Institute of Physics, University of Rostock, Universitätsplatz 3, 18051 Rostock, Federal Republic of Germany
[c] Department of Fundamental Electricity and Instrumentation, Vrije Universiteit Brussel, Pleinlaan 2, 1050 Brussels, Belgium

ARTICLE INFO

Article history:
Received 28 July 2009
Received in revised form
26 October 2009
Accepted 27 October 2009
Available online 4 January 2010

Keywords:
Polymer blend
Phase separation
AC chip calorimetry

ABSTRACT

AC chip calorimetry is used to study the phase separation behavior of 100 nm thin poly(vinyl methyl ether)/poly(styrene) (PVME/PS) blend films. Using the on-chip heaters, very short (10 ms–10 s) temperature jumps into the temperature window of phase separation are applied, simulating laser heating induced patterning. These temperature pulses produce a measurable shift in the glass transition temperature, evidencing phase separation. The effect of pulse length and height on phase separation can be studied. The thus phase separated PVME/PS thin films remix rapidly, in contrast with measurements in bulk. AC chip calorimetry seems to be a more sensitive technique than atomic force microscopy to detect the early stages of phase separation in polymer blend thin films.

1. Introduction

Polymer blend thin films are interesting both for their technological applications (e.g. coatings, …), and from an academic point of view. By confining a polymer (blend) in a thin film, both the air-polymer and the polymer–substrate interface can (significantly) influence its physical properties, in comparison with those observed in bulk. For polymer blends, increasing and decreasing cloud point temperatures [1,2] and changes in the phase separation mechanism have been reported [3–9]. One of the applications of polymer blend thin films are the so called *'smart surfaces'*, whose properties change as a result of phase separation by thermal stimuli, e.g. the patterning of polymer blend films by local heating. The idea is to use a polymer blend film, which is stable at the storage/working temperature, but can be annealed in the two-phase region upon heating. For patterning, local heating could, for instance, be obtained using an infrared laser. However, two questions arise; firstly, can there be phase separation at the typically very short irradiation times (μs to ms) and secondly, is the resulting morphology stable?

Modulated temperature differential scanning calorimetry (MTDSC) has proven to be a valuable technique for studying phase separation in polymer blends and solutions. MTDSC allows the measurement of accurate glass transition temperatures at low heating rates. Scanning experiments and quasi-isothermal experiments enable the monitoring of demixing and remixing kinetics of polymer mixtures by following the apparent heat capacity signal [10–18]. However, the sample mass needs to be rather large (approximately 1 mg), hampering the study of thin films. Chip based nano calorimetry could allow the calorimetric study of phase separation in thin films. In literature, two approaches for nano calorimetry are reported: a quasi-adiabatic approach, as developed by Allen et al. [19–22], and a non-adiabatic one, as developed by Schick et al. [23–29].

In this paper, polymer blend thin films are studied using a non-adiabatic differential AC chip calorimeter. The poly(vinyl methyl ether)/poly(styrene) (PVME/PS) blend system was chosen as a model system. PVME/PS blend thin films have been studied in detail in literature [1–7,30–34] and show a lower critical solution temperature (LCST) behavior, i.e. starting from a homogeneous system, they will phase separate above a certain temperature. The ability of differential AC chip calorimetry to study phase separation in thin PVME/PS blend films is evaluated. The phase separation behavior in bulk is compared with that of 100 nm thin films. Furthermore, the on-chip heater is used to apply heating pulses from the homogeneous to the two-phase region of the state diagram and this for very short durations (10 ms to several seconds). This allows the study of the phase separation kinetics on

* Corresponding author. Tel.: +32 2 629 32 76; fax: +32 2 629 32 78.
E-mail address: bvmele@vub.ac.be (B. Van Mele).

0032-3861/$ – see front matter © 2010 Elsevier Ltd. All rights reserved.
doi:10.1016/j.polymer.2009.10.062

the ms–s time scale, thus simulating laser heating induced patterning.

2. Experimental

2.1. Materials

PS with a molar mass (M_w) of 344.000 g/mol, a polydispersity index (PI) of 3.33, and a glass transition temperature (T_g) of 105 °C, is a commercial product from Aldrich Chemical Company Inc. PVME was purchased as an aqueous solution (50 wt%) from Aldrich Chemical Company Inc. and has a M_w of 60.000 g/mol, a PI of 3, and a T_g of −27 °C.

2.2. Film preparation

PVME was dried under vacuum at 40 °C for 48 h. All blend compositions were dissolved in toluene with an overall polymer concentration of 2 wt%. Films with a uniform thickness of approximately 100 nm were obtained by spin coating at 2000 rpm. The film thickness was verified using ellipsometry and atomic force microscopy (AFM).

2.3. Optical microscopy

Bulk cloud points were detected by measuring the light transmitted through 1 mm thick samples between glass slides in a Mettler Toledo FP82HT hot stage equipped with a photodetector. A Spectratech optical microscope was used with a magnification of 4 and a light source operating with visible light. All samples were heated at a rate of 1 K min^{-1} to reduce thermal lag in the sample and to allow comparison with MTDSC measurements at a similar underlying heating rate. The onset of the decrease in the transmitted light intensity was chosen as the cloud point temperature.

2.4. Modulated temperature differential scanning calorimetry

MTDSC measurements were performed on a helium purged (25 ml min^{-1}) TA Instruments 2920 DSC with MDSC™ option equipped with a refrigerated cooling system (RCS). Temperature and enthalpy calibration were performed using an indium standard. Unless stated otherwise, measurement conditions were an underlying heating rate of 2.5 K min^{-1} with an applied temperature modulation of 0.5 K/60 s. Samples were pretreated under vacuum at 80 °C, below the expected cloud point of the blend, prior to the introduction into the DSC. Non-hermetic aluminum crucibles (Perkin Elmer) were used.

2.5. AC chip calorimetry

A Xensor Integration XI 295 sensor was used (see Fig. 1). The sensors are made of a 500 nm thick silicon nitride membrane. Two poly-silicon heaters (1) supply the necessary heating power in order to obtain a homogeneous temperature distribution over the heated area (60 × 70 μm) [35]. The temperature of the sample is recorded with a six-junction thermopile (2) located in the center of the heated area. The membrane, the conducting stripes, heaters and thermopile are covered with a 800 nm chemical vapor deposited silicon oxide layer.

In differential AC chip calorimetry, the heat capacity of the sample is given by:

$$C_s(\omega) = \frac{i\omega(C_0 + G/i\omega)^2(\Delta U - \Delta U_0)}{SP_0} \quad (1)$$

with i the imaginary unit, ω the angular frequency, $C_0(\omega)$ the heat capacity of the empty sensor, $G/i\omega$ the heat loss through the membrane and the surrounding gas, S the thermopile sensitivity, P_0 the amplitude of the applied power, ΔU the differential voltage amplitude from the combination of an empty sensor and a sensor with sample, and ΔU_0 the differential voltage amplitude from two empty sensors.

At the glass transition, the effective heat capacity of the sample sensor and, consequently, the thermopile voltage slowly varies. As a result, the change of sample heat capacity at the glass transition can be estimated by:

$$\Delta C_S(\omega) = C_S^{liquid}(\omega) - C_S^{glass}(\omega) = \frac{i\omega(C_0 + G/i\omega)^2(\Delta U(l) - \Delta U(g))}{SP_0} \quad (2)$$

In all following experiments, the differential voltage amplitude ΔU is plotted versus temperature and indicative for the heat capacity variation. The underlying heating/cooling rate of the thermostat is 2 K min^{-1} for the construction of the state diagram and 5 K min^{-1} for the pulsed measurements, with a temperature modulation of 0.4 K/12.5 ms (80 Hz). All measurements were performed under nitrogen at ambient pressure, in order to avoid thermal degradation. Standard cleaning conditions of the sensors consisted in a droplet of acetone evaporated by spinning to remove dust and organic contaminants. A second droplet was applied for +/−10 s in order to dissolve the remaining contaminants. This procedure was repeated three times, followed by heating under vacuum at 200 °C for 2 h. This heating step was necessary to fully cure the epoxy resin used to glue the chip to the housing. The quality of the surface clean was checked using AFM.

2.6. Atomic force microscopy

The cloud point temperatures of the 100 nm films were determined using a Topometrix Explorer AFM. Topographic and friction images were recorded in contact mode (Topometrix contact AFM-1520 Si_3N_4 tip, spring constant 28 N/m). For this study, all blend compositions were spincoated on silicon wafers (natural oxide layer), which were previously cleaned following the same cleaning procedure as the AC chip calorimeter sensors. Each sample was annealed for 15 min at high temperature in a vacuum furnace. The temperature was increased stepwise with 1° until the onset of domain formation was observed.

Morphological information was obtained in tapping mode using an Asylum Research MFP-3D AFM. Topographic and phase images were recorded at room temperature using an Olympus AC 160TM cantilever (Resonance frequency 300 kHz, spring constant 42 N/m). Typical scan rates were between 0.4 and 1 Hz.

In order to visualize the morphology produced by the temperature jumps inside the temperature window of phase separation, a special setup was built. This setup allowed the visualization of the sensor surface when coupled to an arbitrary wave function generator, making it possible to image the surface immediately after applying a temperature jump. More details can be found in the results and discussion section.

3. Results and discussion

3.1. Methodology

In AC chip calorimetry the total mass of sensor and sample is very low in comparison with (MT)DSC. Hence, a new methodology to study phase separation could be developed. In a first (slow) scanning experiment, the homogeneous blend film is

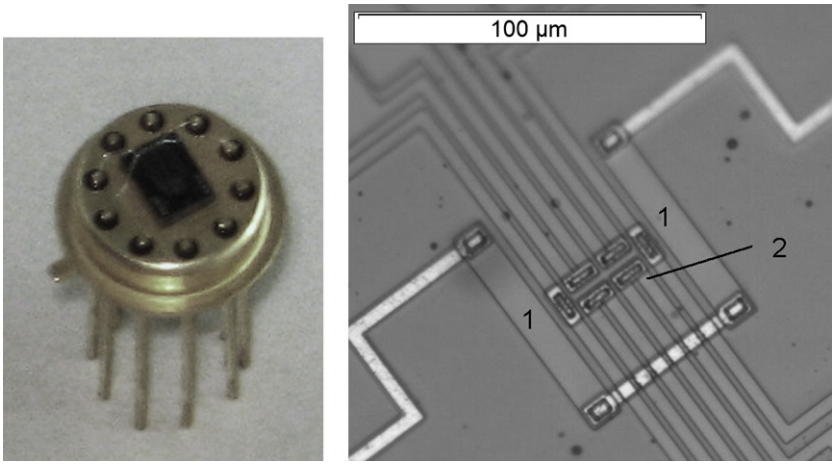

Fig. 1. (Left) The typical TO5 housing used for AC chip calorimetry. (Right) Optical microscopy image of the heated area (60 × 70 µm) of a Xensor Integration XI-295 chip. The six thermocouples in the center of the heated area are visible, just as the two heater stripes.

characterized. The sample is cooled down below the glass transition temperature of the low T_g component in the blend (PVME). While the furnace is kept at this low temperature, a temperature jump, towards a temperature above the cloud point temperature (T_{cl}), is applied to the sample using the on-chip heaters. The length of this pulse segment typically ranges from 10 ms up to 10 s. The sample is again quenched to the temperature of the furnace, freezing the thus obtained morphology. In a second slow scanning experiment the influence of the temperature jump is measured. During this second scanning experiment the sample can remix progressively. Hence, only the glass transition temperature of the phase, rich in the low T_g component (PVME-rich phase), will be unaffected by the remixing during the slow scanning and will illustrate the influence of the temperature jump above the cloud point temperature. The applied temperature program is depicted schematically in Fig. 2.

Once the cloud point temperatures are determined, this methodology allows the study of phase separation processes in the millisecond range and will be a valuable tool to simulate the influence of very short localized heating, as obtained in a laser heating experiment. By varying the pulse length and/or pulse temperature, information can be gathered about the kinetics and mechanism of the phase separation and the possible degradation at higher temperatures.

The temperature evolution for a typical heating pulse experiment is displayed in Fig. 3. In this experiment a pulse with a length of 1 s and a height of 175 °C is applied. The observed noise in the temperature signal is due to the limited sensitivity of the ADC of the digital oscilloscope used and does not correspond to stability of temperature, which is better than 1 K. The time constant τ in heating equals 5 ms, whereas the cooling is somewhat slower ($\tau = 7$ ms). This 5 ms time constant restricts the lower limit of the pulse length to 10 ms.

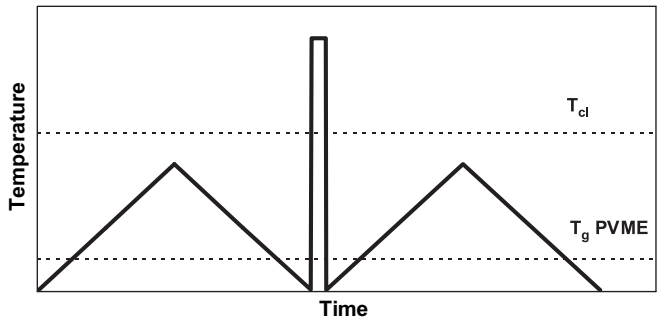

Fig. 2. Schematic diagram of a typical AC chip calorimeter experiment. The homogeneous polymer blend is characterized in the first slow scanning experiment. The influence of the temperature jump is measured in the second heating.

3.2. State diagram of PVME/PS thin films

Prior to the temperature jump experiments, the state diagram is constructed for PVME/PS in 100 nm films on silicon oxide (Fig. 4) in order to delimit the regions of interest. The homogeneous glass transitions (Δ) were measured using AC chip calorimetry. The cloud point temperatures (□) of the 100 nm films were determined by contact AFM. Below the cloud point temperature the films are homogeneous. Upon phase separation, the surface of the thin film will roughen and eventually phase domains will be formed [36]. In the case of PVME/PS, distinct differences in topography and friction will appear [9]. PVME-rich domains are characterized by a higher friction and correspond to the holes in the topographic image, as illustrated in Fig. 5 for a PVME/PS 80/20 w/w composition. The cloud point curve determined by AFM is in agreement with the LCST behavior of PVME/PS thin films [2].

3.3. Phase separation by temperature pulses in PVME/PS thin films

The proof of principle of the methodology is illustrated in Fig. 6 for a PVME/PS 70/30 blend. The homogeneous glass transition (13 °C) is measured in both heating and cooling. Fig. 6 also shows the influence of a 10 ms pulse to 150 °C, a temperature clearly inside the two-phase region of the blend. In a subsequent heating scan (see temperature program of Fig. 2), the observed glass transition temperature is lowered to 7 °C and the step change at the glass transition has decreased. This lowered glass transition corresponds to the formation of a PVME-rich phase during the 10 ms pulse. The lower step change at the glass transition is indicative for the existence of the PS-rich phase. Note that the glass transition of the corresponding PS-rich phase is not visible in these experiments. Upon cooling, the system displays again a glass transition temperature of 13 °C with the same step height as in the first heating before the temperature pulse, indicating that it is completely homogenized and has returned to its original state.

Similar results are obtained when a 10 s temperature jump to 105 °C, only slightly above the cloud point temperature, is applied

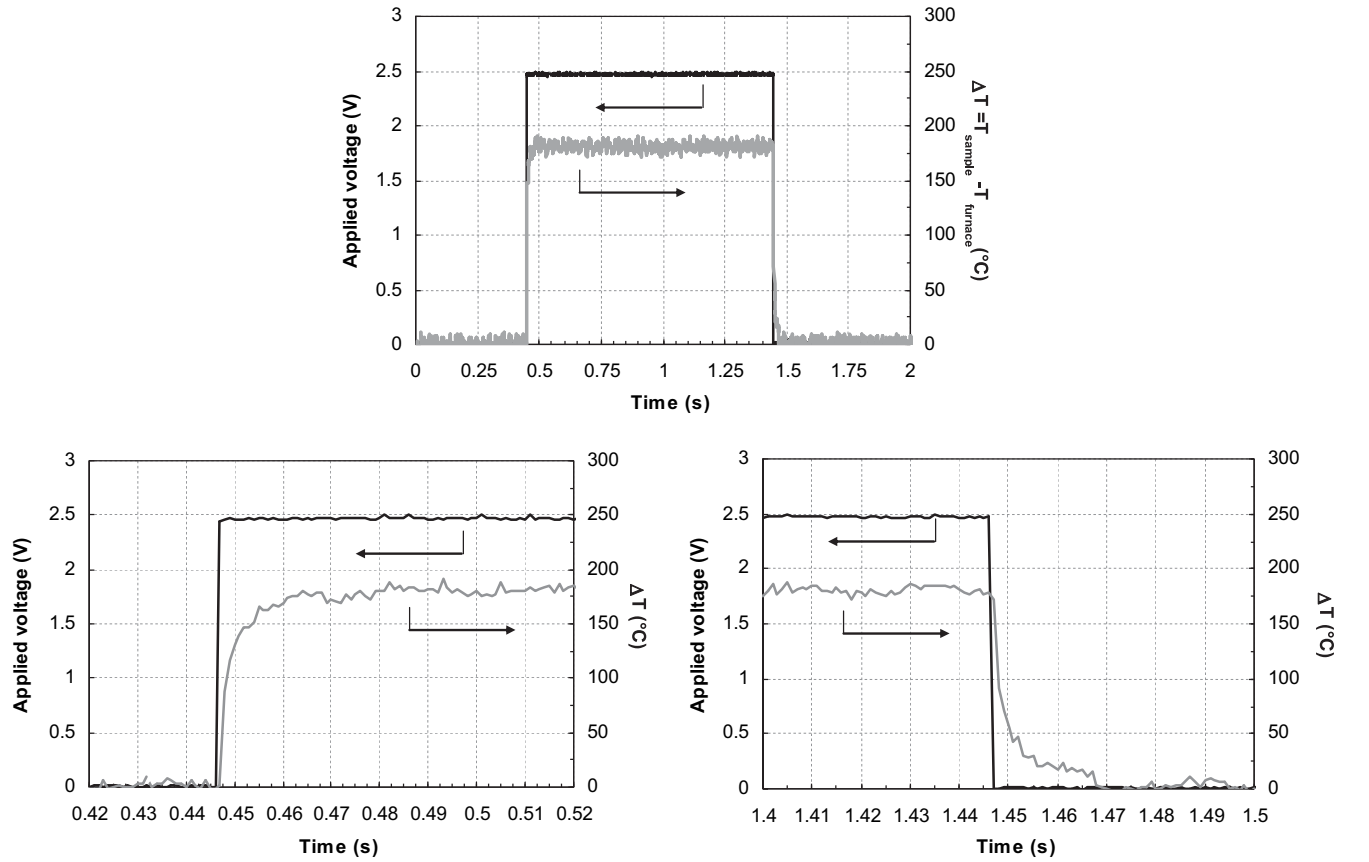

Fig. 3. The applied voltage over the on-chip heater (black) and the measured temperature (grey) are plotted for a 1 s temperature jump to 175 °C. The time constant equals 5 ms and 7 ms for heating and cooling, respectively.

(Fig. 7). The glass transition temperature of the PVME-rich phase is lowered to 3 °C and the step change at the glass transition decreases even further. The repeatability of the method is also demonstrated in Fig. 7, as a second identical pulse results in the same findings as for the first pulse. Figs. 6 and 7 clearly indicate that the applied methodology is not only reproducible, but also allows consecutive measurements of different pulse temperatures and pulse lengths while using the same spincoated sample on the chip, each time restarting from the homogeneous state of the sample.

3.4. Influence of pulse length and height

The method described above is applied to investigate the influence of the time spent above the cloud point temperature for a PVME/PS 70/30 mixture. The pulse temperature is fixed at 150 °C and the pulse length is varied from 10 ms up to 5 s. Fig. 8 shows that, with increasing pulse length, the glass transition temperature of the PVME-rich phase evolves towards that of the equilibrium composition at 150 °C (left arrow). The decrease in relaxation strength at the glass transition temperatures of the PVME-rich and PS-rich (not shown) phases, illustrates the changing composition of the interphase (right arrow). The influence of the first pulse (10 ms) is large in comparison with the 100 times longer 1 s pulse, indicating that the phase separation process is very fast. Especially the value of T_g of the PVME-rich phase is influenced in the early stage of phase separation (left arrow), while the interphase region is still changing significantly in the later stages (right arrow). A tentative explanation might be a spinodal decomposition phase separation mechanism with compositional phase changes in the early stages

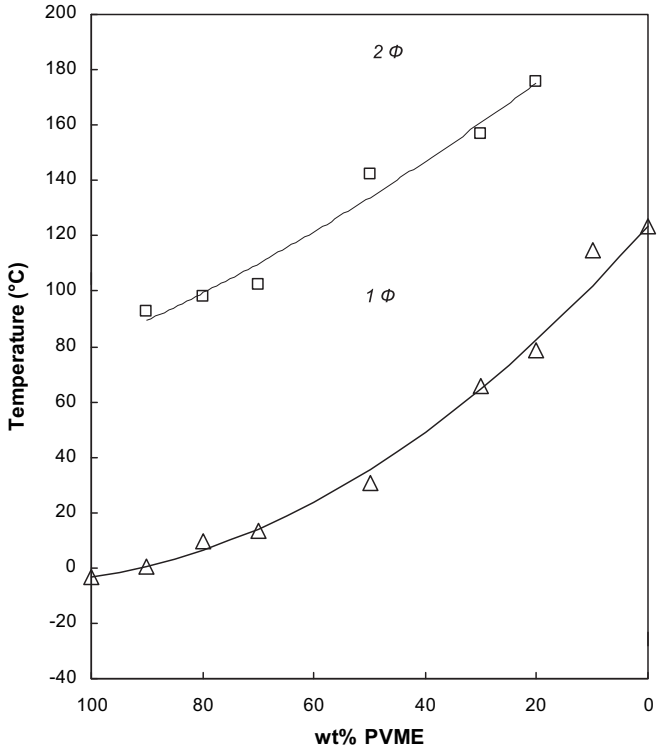

Fig. 4. State diagram of PVME/PS in 100 nm films on silicon oxide. The cloud points are determined using AFM (□). The homogeneous glass transition temperatures are measured using AC chip calorimetry (Δ).

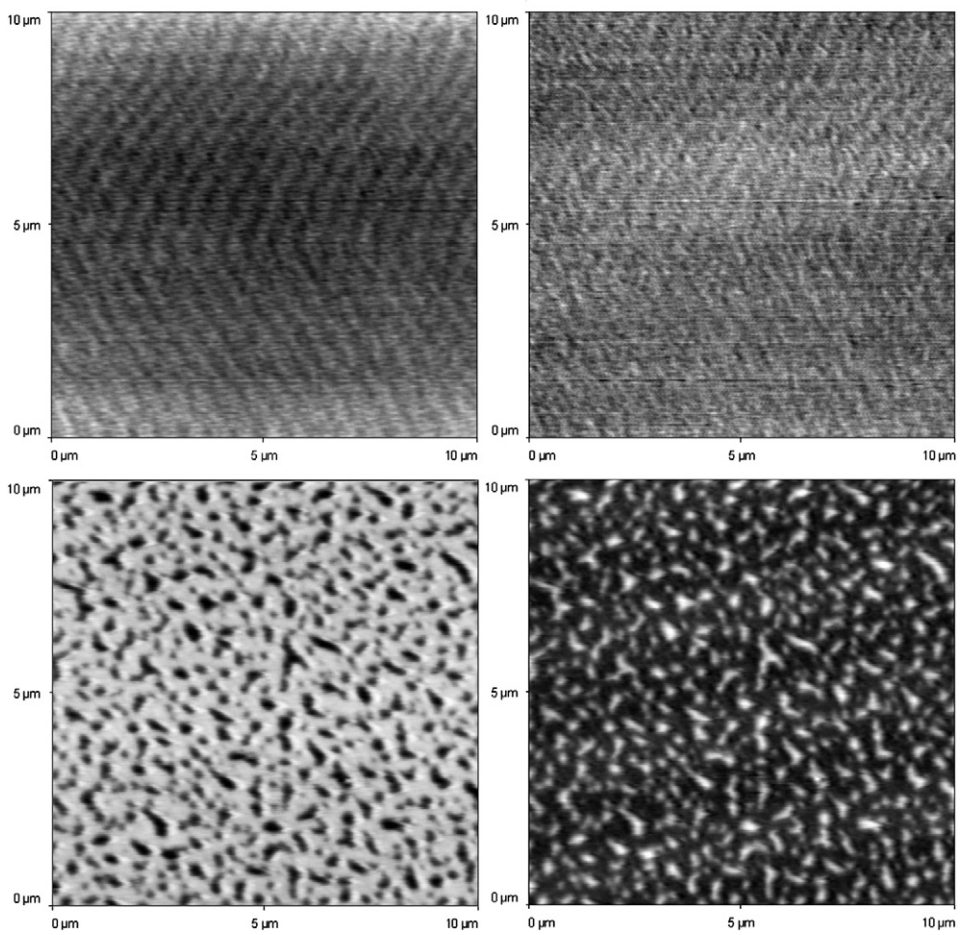

Fig. 5. Determination of the cloud point temperature for a PVME/PS 80/20 blend film using contact AFM. Topographic (left) and friction (right) images are shown at room temperature (top) and after 15 min annealing at the cloud point temperature (bottom).

and coarsening of phases in the later stages. More research is needed to elucidate these effects.

In order to simulate laser patterning, the influence of the amplitude of the temperature jump for a fixed pulse length on a PVME/PS 70/30 mixture is shown in Fig. 9. Pulse temperatures are varied from 150° up to 330 °C with a fixed pulse length of 10 ms.

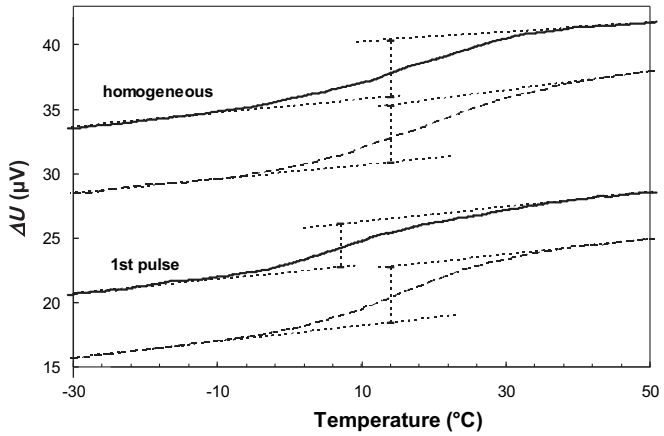

Fig. 6. Differential amplitude of the thermopile signal in a heating (full) and cooling (dashed) sequence for a PVME/PS 70/30 nm film. The upper two curves show the homogeneous system, the lower two curves the influence of a preceding 10 ms pulse to 150 °C (see the temperature program of Fig. 2). In the cooling scan the system is again homogenized. Note that the curves are shifted vertically for clarity.

For pulses below 150 °C no phase separation is observed and the homogeneous glass transition temperature is found. For pulses from 150° to 264 °C, a shift in the glass transition temperature of the low T_g (PVME-rich) phase towards that of pure PVME is

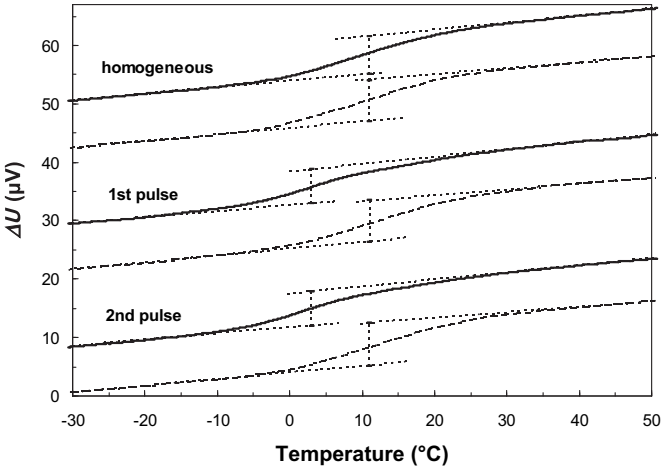

Fig. 7. Differential amplitude of the thermopile signal in a heating (full) and cooling (dashed) sequence for a PVME/PS 70/30 nm film. The upper two curves show the homogeneous system, the other curves the influence of a preceding 10 s pulse to 105 °C. In the cooling scan the system is again homogenized. The repeatability is demonstrated for two successive pulses. Note that the curves are shifted vertically for clarity.

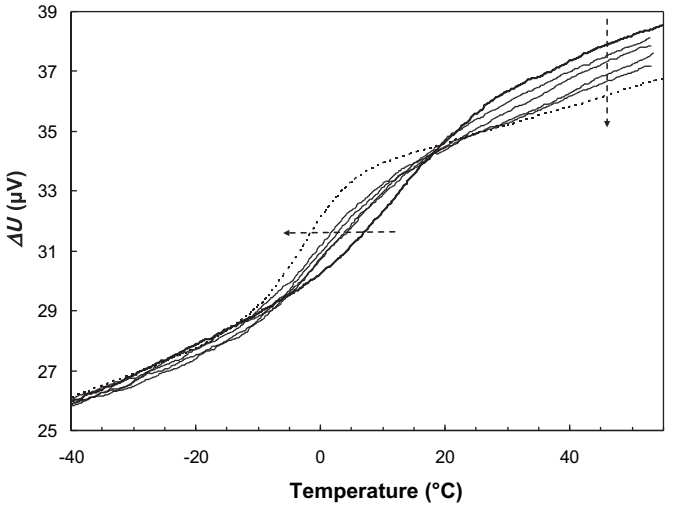

Fig. 8. Differential amplitude of the thermopile signal for a PVME/PS 70/30 blend after one pulse to 150 °C with a pulse length of 10 ms, 100 ms, 1 s and 5 s. The arrows indicate the increase in pulse length starting from the homogeneous blend (full). The curve around T_g of pure PVME (dotted), calculated for a 70/30 blend composition, considering pure co-existing phases, is added for comparison.

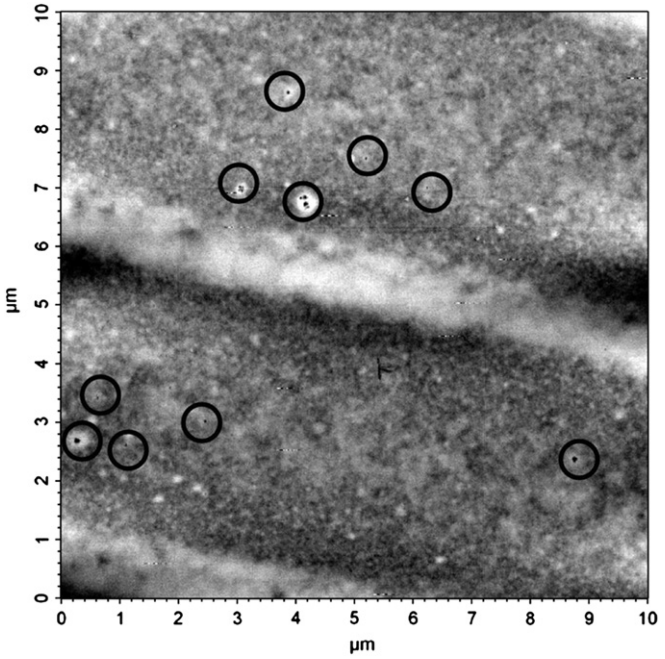

Fig. 10. Tapping mode AFM phase image (10 × 10 μm) measured at 30 °C of a 100 nm PVME/PS 30/70 blend film on a Xensor Integration XI-295 sensor after heating 10 s at 175 °C using the on-chip heaters.

evidenced. The changing composition of the PVME-rich phase, for temperatures up to 264 °C, reflects the shape of the LCST curve. Above 264 °C the T_g of the PVME-rich phase remains constant. Another explanation might be the observations of Wang et al. They demonstrated that, as the film thickness of a polymer blend is between the radius of gyration (R_g) and 10 times R_g, which is the case in the present study, one might expect that the initial stage of the phase separation corresponds to the development of a trilayer structure [37]. However, as the middle layer is too thin to support long wavelength fluctuations, the correlated holes will develop along thinned regions of the middle layer and these holes grow and coalesce into a network structure. This would mean that during a 10 ms temperature jump, the breaking of the middle layer is only observed for temperatures above 264 °C, while the development of the trilayer structure is observed for pulses up to 264 °C. To underpin this tentative explanation, however, further experiments are required.

This experiment allows the study of a possible degradation at high temperature, as PVME and PS start to degrade at approximately 180 °C in slow heating thermogravimetric analysis conditions. However, in AC calorimetry with 10 ms temperature pulses there are no signs of thermal degradation; a good signal is obtained even for heating pulses up to 330 °C. Moreover, the homogeneous glass transition temperature is found with a constant step change upon cooling after all pulses applied, confirming that no degradation occurred even for (short) pulses at the highest temperatures.

AC chip calorimetry gives insight in the composition of the co-existing phases upon phase separation. Morphological information, however, can not be obtained. This shortcoming can be circumvented by combining AC chip calorimetry with atomic force

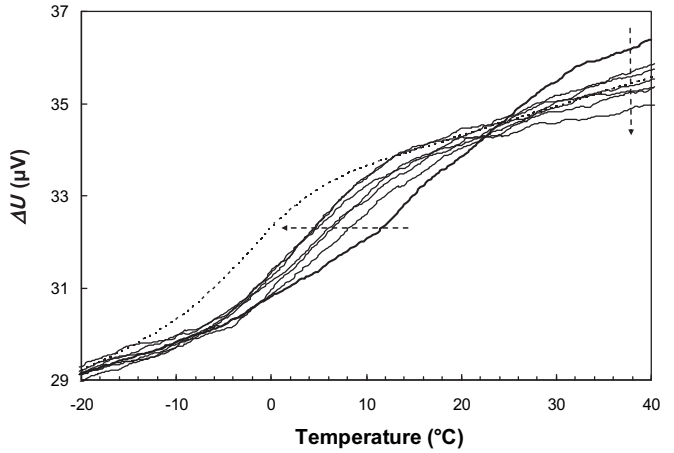

Fig. 9. Differential amplitude of the thermopile signal for a PVME/PS 70/30 blend after a 10 ms pulse to 150, 205, 233, 264, 297 and 330 °C. The arrows indicate the increase of the demixing temperature starting from the homogeneous blend (full). The curve around T_g for pure PVME (dotted), calculated for a 70/30 blend composition considering pure co-existing phases, is added for comparison.

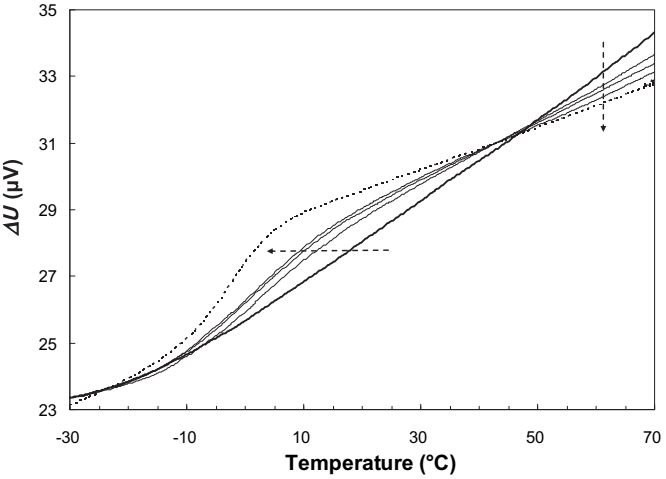

Fig. 11. Differential amplitude of the thermopile signal for a PVME/PS 30/70 blend after a 1 s pulse to 150, 175 and 204 °C. The dashed arrows indicate the increase of the demixing temperature starting from the homogeneous blend (full). The curve around T_g for pure PVME (dotted), calculated for a 30/70 blend composition considering pure co-existing phases, is added for comparison.

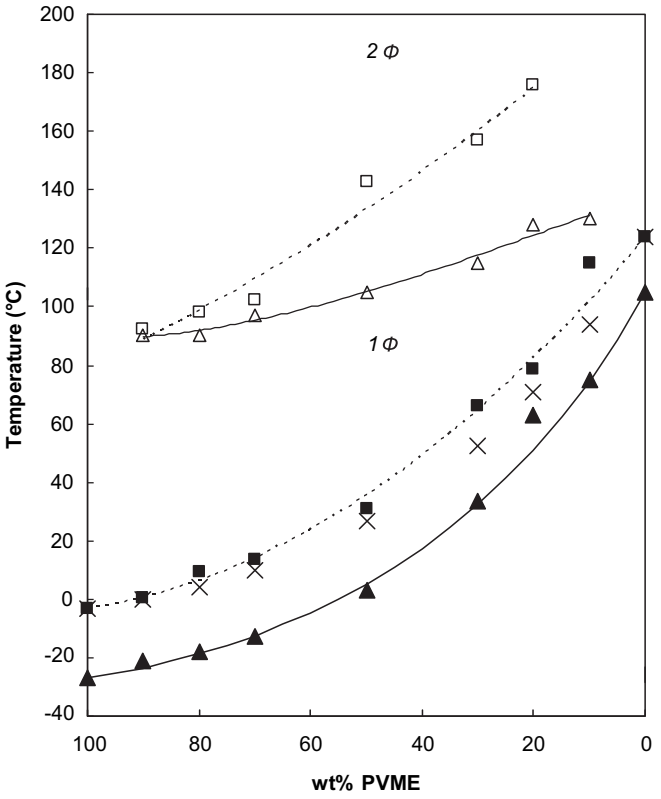

Fig. 12. State diagram for PVME/PS in bulk and in a 100 nm film on silicon oxide. Bulk cloud point temperatures were determined by optical microscopy (Δ). Bulk homogeneous glass transition temperatures (▲) were measured using MTDSC and fitted with the equation of Kwei with $k_{KW} = 0.41$ and $q_{KW} = -24$. Thin film cloud point temperatures were determined by contact AFM (□). Thin film homogeneous glass transition temperatures (■) were measured using AC chip calorimetry and fitted with the equation of Kwei with $k_{KW} = 1$ and $q_{KW} = -99$. The shift in bulk T_g due to the measurement frequency, interpolated for all compositions using the observed shift for pure PVME and PS, is added for clarity (×). The cloud point curves are a guide to the eye.

microscopy. For this purpose, a special setup was built and placed under the AFM. This setup allows the scanning of the sensor surface while being coupled with an arbitrary wave function generator. Hence, the same pulses as in AC chip calorimetry can be applied to the sample while its corresponding morphology is visualized.

Starting from a homogeneous PVME/PS 30/70 film, tapping mode AFM images were recorded after heating in the heterogeneous region for 1 s to different temperatures. No phase separation was observed for pulses to temperatures below 175 °C. For pulses above 175 °C, the onset of surface roughening is observed. By increasing the pulse length to 10 s, small circular domains of approximately 100 nm diameter appear (Fig. 10). Remixing, evidenced by the disappearance of the circular domains, is observed upon annealing at 40 °C in the homogeneous region of the phase diagram.

Using AC chip calorimetry an analogous experiment is performed. The effect of 1 s pulses with increasing pulse heights on a PVME/PS 30/70 film is investigated. From Fig. 11, it is clear that 1 s pulses to 150 °C, 175 °C and 204 °C influence the T_g of the PVME-rich phase. Hence, AC chip calorimetry is a more sensitive technique than AFM to study the early stages of the phase separation.

3.5. Comparison with phase separation of PVME/PS in bulk

It is well known from literature that in a polymer blend thin film, both the air-polymer and the substrate–polymer interface can alter the phase separation temperature and/or mechanism [1–9].

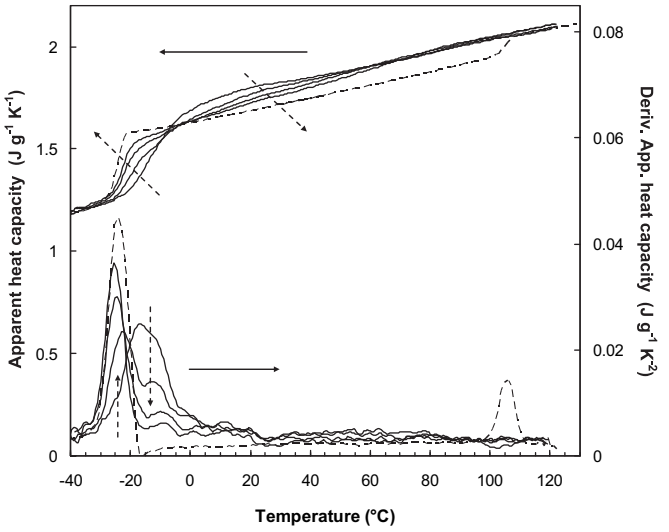

Fig. 13. Apparent heat capacity of MTDSC and its temperature derivative for a PVME/PS 70/30 bulk blend after increasing demixing times at 130 °C: 0 min (homogeneous), 1, 10, and 30 min. The dashed arrows indicate the increase of the demixing time. T_g for pure PVME and PS, calculated for a 70/30 blend composition, is added for comparison (dashed).

Fig. 12 shows the differences between the state diagram of PVME/PS in 100 nm films on silicon oxide and in bulk. The cloud point temperatures are shifted to higher values for the thin films. It should be noted that the cloud points for thin films and bulk are characterized by means of different techniques, AFM and optical microscopy, respectively. The shift in the observed glass transition temperature of the thin films is largely due to the higher measurement frequency in AC chip calorimetry. The frequency dependence of T_g can be fitted using a WLF equation [38], as was illustrated in [39] for PS and PMMA. Using the parameters from [39] for pure PS, a shift of 19 K, due to the difference in measurement frequency between MTDSC (17 mHz) and AC chip calorimetry (80 Hz), can be calculated, in accordance to our measurements. The observed shift in T_g for thin films of pure PVME and for intermediate blend compositions is larger than for pure PS. The observed shift for pure PS and pure PVME can be used to interpolate the shift for

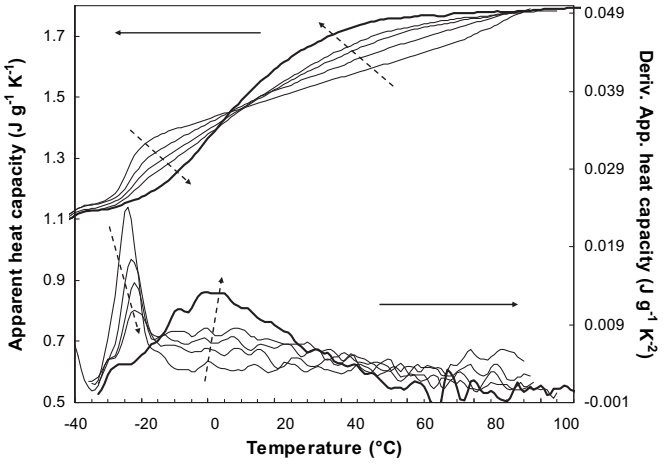

Fig. 14. Apparent heat capacity of MTDSC and its temperature derivative for a PVME/PS 50/50 bulk blend demixed for 60 min at 160 °C and remixed at 95 °C for 15, 30, 60 and 240 min towards the homogeneous blend (full). The dashed arrows indicate the increasing remixing time at 95 °C.

intermediate blend compositions (X). The observed shift in T_g for thin films is also larger than these interpolated values for all blend compositions. This might indicate that the film thickness has an influence upon T_g of the thin blend films. The Kwei T_g composition relationship was calculated for the homogeneous blend with $k_{KW} = 1$ and $q_{KW} = -99$ and $k_{KW} = 0.42$ and $q_{KW} = -24$ for thin films and bulk, respectively.

The kinetics of demixing and remixing of the PVME/PS blend in bulk are slow, as can be seen in Figs. 13 and 14. Typical demixing and remixing durations are in the range of minutes for demixing and up to hours for remixing. Fig. 13 shows the influence of the time spent in the heterogeneous region on the subsequent heating, after quenching the sample below T_g of PVME. It is clear that the two phases are progressing towards an almost pure PVME-rich phase and a co-existing PS-rich phase (see also state diagram of Fig. 12). For clarity, the T_g's of the pure components were added after scaling of the ΔC_p at T_g, according to the 70/30 blend ratio, considering pure co-existing phases. The decrease in the derivative of the heat capacity between −20 °C and 100 °C indicates the evolution of the interphase region.

Fig. 14 illustrates the remixing in bulk at 95 °C of a PVME/PS 50/50 blend demixed at 160 °C for 60 min. The remixing process is slow and takes hours for complete homogenization.

It appears that the kinetics of phase separation in thin films are fast compared to bulk. The difference in demixing kinetics might be the result of the film thickness. The difference in remixing, however, is probably a result of the measurement procedure. Due to the very short demixing times in AC chip calorimetry, the obtained morphology (see Fig. 10) is much finer. On the contrary, due to the long demixing times in MTDSC, the contact area between the two phases will be much smaller by coarsening effects, resulting in slower remixing. In order to determine the influence of the film thickness on the phase separation kinetics, more experiments are needed.

4. Conclusions

AC chip calorimetry in combination with AFM was proved to be a powerful tool to study phase separation in thin polymer blend films. A state diagram was constructed for PVME/PS in 100 nm thin films. A new methodology was developed: using the on-chip heaters it was possible to apply very short (10 ms to s) temperature jumps to temperatures above the cloud point temperature, making it possible to simulate laser patterning. Phase separation was evidenced for 10 ms jumps into the two-phase area of the state diagram. The resulting morphology was very fine and remixed very rapidly. AC chip calorimetry using short temperature pulses seems a more sensitive characterization tool than AFM for the detection of the early stages of phase separation in thin polymer films.

Acknowledgments

The Research Foundation Flanders (FWO-Vlaanderen) is kindly acknowledged for supporting this research by a Ph.D. and a post-doctoral research grant. The authors are grateful to C. de Tandt (Dept. of Electronics and Informatics, Vrije Universiteit Brussel) for giving access to and assistance with the spincoater.

References

[1] Reich S, Cohen Y. Journal of Polymer Science: Polymer Physics Edition 1981;19(8):1255–67.
[2] Tanaka K, Yoon J-S, Takahara A, Kajiyama T. Macromolecules 1995;28(4):934–8.
[3] Karim A, Slawecki TM, Kumar SK, Douglas JF, Satija SK, Han CC, et al. Macromolecules 1998;31(3):857–62.
[4] Kawaguchi D, Tanaka K, Kajiyama T, Takahara A, Tasaki S. Macromolecules 2003;36(18):6824–30.
[5] Li X, Wang Z, Cui L, Xing R, Han Y, An L. Surface Science – Including Surface Science Letters 2004;571(13):12–20.
[6] El-Mabrouk K, Belaiche M, Bousmina M. Journal of Colloid and Interface Science 2007;306(2):354–67.
[7] Ogawa H, Kanaya T, Nishida K, Matsuba G. Polymer 2008;49(1):254–62.
[8] Krausch G, Dai CA, Kramer EJ, Bates FS. Berichte der Bunsen-Gesellschaft-Physical Chemistry Chemical Physics 1994;98(3):446–8.
[9] Ermi BD, Karim A, Douglas JF. Journal of Polymer Science, Part B: Polymer Physics Edition 1998;36(1):191–200.
[10] Song M, Hammiche A, Pollock HM, Hourston DJ, Reading M. Polymer 1995;36(17):3313–6.
[11] Song M, Hammiche A, Pollock HM, Hourston DJ, Reading M. Polymer 1996;37(25):5661–5.
[12] Hourston DJ, Song M, Hammiche A, Pollock HM, Reading M. Polymer 1997;38(1):1–7.
[13] Reading M, Hourston DJ. Modulated-temperature differential scanning calorimetry: theoretical and practical applications in polymer characterisation (hot topics in thermal analysis and calorimetry). Springer; 2006.
[14] Dreezen G, Groeninckx G, Swier S, Van Mele B. Polymer 2001;42(4):1449–59.
[15] Swier S, Pieters R, Van Mele B. Polymer 2002;43(13):3611–20.
[16] Van Lokeren L, Gotzen NA, Pieters R, Van Assche G, Biesemans M, Willem R, et al. Chemistry–a European Journal 2009;15(5):1177–85.
[17] Swier S, Van Durme K, Van Mele B. Journal of Polymer Science, Part B: Polymer Physics 2003;41(15):1824–36.
[18] Van Durme K, Van Assche G, Van Mele B. Macromolecules 2004;37(25):9596–605.
[19] Efremov MY, Warren JT, Olson EA, Zhang M, Kwan AT, Allen LH. Macromolecules 2002;35(5):1481–3.
[20] Efremov MY, Olson EA, Zhang M, Lai SL, Schiettekatte F, Zhang ZS, et al. Thermochimica Acta 2004;412(1–2):13–23.
[21] Efremov MY, Olson EA, Zhang M, Zhang Z, Allen LH. Physical Review Letters 2003;91(8):085703.
[22] Efremov MY, Olson EA, Zhang M, Zhang ZS, Allen LH. Macromolecules 2004;37(12):4607–16.
[23] Adamovsky SA, Minakov AA, Schick C. Thermochimica Acta 2003;403(1):55–63.
[24] Adamovsky S, Schick C. Thermochimica Acta 2004;415(1–2):1–7.
[25] Minakov AA, Adamovsky SA, Schick C. Thermochimica Acta 2005;432(2):177–85.
[26] Minakov AA, van Herwaarden AW, Wien W, Wurm A, Schick C. Thermochimica Acta 2007;461(1–2):96–106.
[27] Huth H, Minakov A, Schick C. Netsu Sokutei 2005;32(2):70–6.
[28] Huth H, Minakov AA, Schick C. Journal of Polymer Science, Part B: Polymer Physics 2006;44:2996–3005.
[29] Zhou D, Huth H, Gao Y, Xue G, Schick C. Macromolecules 2008;41(20):7662–6.
[30] Pan DHK, Prest WM. Journal of Applied Physics 1985;58(8):2861–70.
[31] Bhatia QS, Pan DH, Koberstein JT. Macromolecules 1988;21:2166–75.
[32] Dee GT, Sauer BB. Macromolecules 1993;26(11):2771–8.
[33] Lee S, Sung CSP. Macromolecules 2001;34(3):599–604.
[34] Pavawongsak S, Higgins JS, Clarke N, McLeish TCB, Peiffer DG. Polymer 2000;41:757–63.
[35] Minakov A, Morikawa J, Hashimoto T, Huth H, Schick C. Measurement Science and Technology 2006;17(1):199–207.
[36] Wang H, Composto RJ. Europhysics Letters 2000;50(5):622–7.
[37] Wang H, Composto RJ. Interface Science 2003;11(2):237–48.
[38] Weyer S, Hensel A, Schick C. Thermochimica Acta 1997;305:267–75.
[39] Huth H, Minakov AA, Serghei A, Kremer F, Schick C. European Physical Journal–Special Topics 2007;141:153–60.